

Massive Overlap Fermions on Anisotropic Lattices¹

Xin Li^a, Guozhan Meng^a, Xu Feng^a, Chuan Liu^a

^a*School of Physics, Peking University
Beijing, 100871, P. R. China*

Abstract

We formulate the massive overlap fermions on anisotropic lattices. We find that the dispersion relation for the overlap fermion resembles the continuum form in the low-momentum region once the bare parameters are properly tuned. The quark self-energy and the quark field renormalization constants are calculated to one-loop in bare lattice perturbation theory. Using tadpole improved perturbation theory, we establish the relation between the well-tuned parameters and the quark mass once the bare coupling is given. We argue that massive domain wall quarks might be helpful in lattice QCD studies on heavy-light hadron spectroscopy.

Key words: massive overlap fermions, anisotropic lattices, lattice perturbation theory.

PACS: 12.38.Gc, 11.15.Ha

1 Introduction

It is known that chiral symmetry plays an essential role in low-energy Quantum Chromodynamics (QCD), which is believed to be the underlying fundamental theory for strong interactions. Another predominant feature for low-energy QCD is its non-perturbative nature. Lattice QCD provides a genuine non-perturbative theoretical framework for the study of low-energy QCD from first principles. Chirality is associated with masslessness of fermions. Incorporating massless fermions have always been a great challenge in lattice studies

¹ This work is supported by the Key Project of National Natural Science Foundation of China (NSFC) under grant No. 10235040, No. 10421003, No. 10675005 and supported by the Trans-century fund and the Key Grant Project of Chinese Ministry of Education (No. 305001).

due to both theoretical and numerical difficulties. In recent years, considerable progress has been made in understanding chiral symmetry on the lattice. Domain wall fermions [1,2] and the overlap fermions [3,4,5,6,7] have emerged as two new candidates in the formulation of lattice fermions which have much better chiral properties than the conventional Wilson or staggered fermions. Since chiral symmetry is so crucial to the theory of QCD, it is therefore desirable to use these new fermions if possible.

On the other hand, anisotropic lattices have been used extensively on heavy hadronic states and they proved to be extremely helpful in various applications. These include: glueball spectrum calculations [8,9,10], charmonium spectrum calculations [11,12], charmed meson and charmed baryon calculations [13,14] and hadron-hadron scattering calculations [15,16,17,18]. Note that many of the above mentioned studies involve light quarks for which chiral symmetry is essential. It is therefore desirable to use either domain wall or overlap fermions which have better chiral properties. Indeed, much of the systematic uncertainties in these studies originates from chiral extrapolations. It is therefore tempting to study the new lattice fermions (domain wall fermions or overlap fermions) on four-dimensional anisotropic lattices. In a previous study, we have formulated domain wall fermion on anisotropic lattices using bare perturbation theory to one-loop order [19]. In this paper, we will perform a similar study for the overlap fermions. These studies provide us with some guiding information on the tuning of the parameters in the corresponding fermion action which is necessary in realistic Monte Carlo simulations.

In this paper, we study massive overlap fermions on anisotropic four-dimensional lattices. For the gauge action, we adopt the tadpole improved gauge actions [20,8] which have been used in various lattice calculations. The fermion action on anisotropic lattices generally contains more parameters than its isotropic counterparts. These parameters have to be tuned properly in order to yield a correct continuum limit. We will first address this issue in the case of free overlap fermions on anisotropic lattices. It is found that, in order to restore the normal relativistic dispersion relation for the quark, parameters of the fermion action have to be tuned accordingly. Then, we compute the quark propagator in lattice perturbation theory to one-loop. Quark field and quark mass renormalization constants are obtained for various values of the bare parameters. This perturbative calculation serves as a guidance for further non-perturbative Monte Carlo simulations. Similar perturbative calculations have been performed in the case of isotropic lattice [21,22,23,24]. Our calculation is an extension of these to the case of anisotropic lattice. The use of both anisotropic lattices and overlap fermions to treat relativistic heavy quarks on the lattice was first advocated in Ref. [25] where the authors have considered the dispersion relation of quarks in a quenched numerical study.

This paper is organized as follows. In section 2, overlap fermion action on

anisotropic lattices is given. In section 3, the free overlap fermion propagator on anisotropic lattices is presented and the dispersion relation of the free overlap fermion is studied. It is found that hopping parameters of the fermion action have to be tuned properly, according to the value of the bare quark mass, so as to have the correct continuum limit for the massive quark. In section 4, the calculations of fermion self-energy to one-loop is presented. Numerical results for the renormalization factors for the quark field and the current quark mass are listed. In section 5, we will conclude with some remarks and outlook. The one-gluon and two-gluon vertex functions are listed in the appendix.

2 The overlap fermions on anisotropic lattices

The fermion action for the exact massless overlap quark has the following form [5,6,7]:

$$S_F = \sum_{x,y} \bar{\psi}(x) D_{xy} \psi(y), \quad (1)$$

with the (massless) overlap Dirac operator given by:

$$D(m = 0) = \left(1 + X \frac{1}{\sqrt{X^\dagger X}} \right). \quad (2)$$

The operator X appearing in the above equation is the Wilson-Dirac operator on anisotropic lattices which we write as:

$$\begin{aligned} X_{xy} = & \frac{1}{2} \sum_{\mu=1}^4 \kappa_\mu \left[\gamma_\mu \left\{ \delta_{x+\hat{\mu},y} U_\mu(x) - \delta_{x,y+\hat{\mu}} U_\mu^\dagger(y) \right\} \right. \\ & \left. + r_\mu \left\{ 2\delta_{x,y} - \delta_{x+\mu,y} U_\mu(x) - \delta_{x,y+\mu} U_\mu^\dagger(y) \right\} \right] + M_0 \delta_{x,y}, \end{aligned} \quad (3)$$

where r_μ represents Wilson parameters introduced to remove the doublers from low-energy spectrum. In the case of anisotropic lattice, we will also use the convention: $r_0 = r_t$, $r_i = r_s$. The parameter M_0 is usually taken to be negative so as to restore chiral properties of the quark. Since one can scale the operator X by a constant factor without changing fermion matrix D , one might just fix the parameter κ_s to some constant, say +1. We will also set the temporal Wilson parameter $r_t = 1$. It is well-known that the massless overlap Dirac operator $D(m = 0)$ satisfies the Ginsparg-Wilson relation [26] which can be viewed as a generalization of the continuum chiral symmetry to the lattice [27,28]. The Dirac operator also has a massless mode which has definite chirality.

For the massive quarks, one has to modify the massless overlap Dirac operator

given in (2) to [5]:

$$D(m) = \left(1 + \frac{m}{2} + \left(1 - \frac{m}{2} \right) X \frac{1}{\sqrt{X^\dagger X}} \right). \quad (4)$$

It is known that the chiral mode then acquires a mass that is proportional to the parameter m for small values of m . With these conventions, the lattice action describing a massive domain wall fermion depends on 4 bare parameters: the Wilson mass parameter M_0 , the temporal hopping parameter κ_t , the spatial Wilson parameter r_s and the bare quark mass parameter m .

In perturbation theory, it is convenient to study these matrices in Fourier space. After Fourier transformation of the matrix X :

$$X_{xy} = \int_{-\pi}^{\pi} \frac{d^4 p}{(2\pi)^4} \frac{d^4 q}{(2\pi)^4} e^{i(qx-py)} \tilde{X}(q, p), \quad (5)$$

the quantity $\tilde{X}(q, p)$ is expanded into power series in the bare coupling g_0 :

$$\tilde{X}(q, p) = \tilde{X}_0(p)(2\pi)^4 \delta_P(q - p) + \tilde{X}_1(q, p) + \tilde{X}_2(q, p) + O(g_0^3), \quad (6)$$

where the functions \tilde{X}_i are of the order of $(g_0)^i$ respectively. Higher order contributions are not needed in an one-loop calculation. The explicit expressions are found to be:

$$\begin{aligned} \tilde{X}_0(p) &= i\cancel{p} + \sum_{\mu} \kappa_{\mu} r_{\mu} (1 - \cos p_{\mu}) + M_0, \\ \tilde{X}_1(q, p) &= \sum_{A, \mu} \int \frac{d^4 k}{(2\pi)^2} (2\pi)^4 \delta_P(q - p - k) \times g_0 A_{\mu}^A(k) T^A V_{1\mu} \left(p + \frac{k}{2} \right), \\ \tilde{X}_2(q, p) &= \sum_{A, B, \mu, \nu} \int_{-\pi}^{\pi} \frac{d^4 k_1}{(2\pi)^4} \frac{d^4 k_2}{(2\pi)^4} (2\pi)^4 \delta_P(q - p - \sum k_i) \\ &\quad \times \frac{g^2}{2} A_{\mu}^A(k_1) A_{\nu}^B(k_2) T^A T^B V_{2\mu} \left(p + \frac{\sum k_i}{2} \right), \end{aligned} \quad (7)$$

where $\cancel{p} = \sum_{\mu} \kappa_{\mu} \gamma_{\mu} \sin p_{\mu}$ and the functions $V_{1\mu}$ and $V_{2\mu}$ are given by:

$$\begin{aligned} V_{1\mu} \left(p + \frac{k}{2} \right) &= \kappa_{\mu} \left(i\gamma_{\mu} \cos \left(p + \frac{k}{2} \right)_{\mu} + r_{\mu} \sin \left(p + \frac{k}{2} \right)_{\mu} \right), \\ V_{2\mu} \left(p + \frac{\sum k_i}{2} \right) &= \kappa_{\mu} \left(-i\gamma_{\mu} \sin \left(p + \frac{\sum k_i}{2} \right)_{\mu} + r_{\mu} \cos \left(p + \frac{\sum k_i}{2} \right)_{\mu} \right). \end{aligned} \quad (8)$$

3 Dispersion relation for the free overlap fermions

In this section, we briefly summarize the results for the free overlap fermions on anisotropic lattices. These results can be obtained from their counterparts for the isotropic lattices which can be found from the literature, see for example Ref. [5]. In the free case, we denote the overlap Dirac operator given in Eq. (4) by D_0 . The inverse of D_0 in momentum space is found to be:

$$D_0^{-1}(p) = \frac{1}{2} \frac{\left(1 - \frac{m}{2}\right) X_0^\dagger(p) + \left(1 + \frac{m}{2}\right) \omega(p)}{\left(1 + \frac{m^2}{4}\right) \omega(p) + \left(1 - \frac{m^2}{4}\right) b(p)}, \quad (9a)$$

$$b(p) = \sum_{\mu} \kappa_{\mu} r_{\mu} (1 - \cos p_{\mu}) + M_0, \quad (9b)$$

$$\omega(p) = \sqrt{\tilde{p}^2 + \left(\sum_{\mu} \kappa_{\mu} r_{\mu} (1 - \cos p_{\mu}) + M_0\right)^2} > 0, \quad (9c)$$

where $\tilde{p}^2 = \sum_{\mu} \kappa_{\mu}^2 \sin^2 p_{\mu}$.

The dispersion relation for the physical particle (in this case, a free quark) is obtained by inspecting the time dependence of the propagator in coordinate space:

$$G_0(\mathbf{p}, t) = \int_{-\pi}^{\pi} \frac{dp_0}{2\pi} D_0^{-1}(p_0, \mathbf{p}) e^{ip_0 t}. \quad (10)$$

For large temporal separation t , the above propagator will behave like $e^{-tE_{\mathbf{p}}}$ with $E_{\mathbf{p}}$ being the energy of the particle with three-momentum \mathbf{p} . Using the variable $z = e^{ip_0}$, the above propagator can also be expressed as:

$$G_0(\mathbf{p}, t) = \oint \frac{dz}{2\pi i} z^{t-1} D^{-1}(z, \mathbf{p}). \quad (11)$$

where the contour integral is along the unit circle counter-clockwise. If $D^{-1}(z, \mathbf{p})$ were an entire function of z , the above propagator receives contributions from the poles of $D^{-1}(z)$ within the unit circle. The case for the overlap is a bit more complicated due to the branch cut of $\omega(p)$. However, it can be shown that the leading contribution to the propagator $G_0(t, \mathbf{p})$ at large t comes from the residue of the pole closest to $z = 1$ in the complex z plane. Thus, setting the four-momentum:

$$p_{\mu} = (E_{\mathbf{p}}, \mathbf{p}), \quad (12)$$

and demanding that it is the pole of the propagator $D_0^{-1}(p)$, the above equations yield the relation:

$$-\left(1 + \frac{m^2}{4}\right)^2 \tilde{p}^2 = m^2 b^2. \quad (13)$$

We are only interested in the dispersion relation when the lattice three-momentum

$|\mathbf{p}| \ll 1$. We thus obtain:

$$E_{\mathbf{p}} = E_0 + \frac{\mathbf{p}^2}{2M_{kin}} + O(\mathbf{p}^4), \quad (14)$$

where $E_0 \equiv m_Q$ will be identified as the pole mass of the quark and M_{kin} is the so-called kinetic mass of the quark. After some calculations, the equation satisfied by $E_0 = m_Q$ is found to be:

$$A \cosh^2 E_0 + B \cosh E_0 + C = 0, \quad (15)$$

where the coefficients are given by:

$$\begin{aligned} A &= \kappa_t^2 \left(1 + \frac{m^2}{4}\right)^2 - \kappa_t^2 m^2, \\ B &= 2\kappa_t m^2 (\kappa_t + M_0), \\ C &= -\kappa_t^2 \left(1 + \frac{m^2}{4}\right)^2 - m^2 (\kappa_t + M_0)^2. \end{aligned} \quad (16)$$

It is seen that $E_0 \equiv m_Q$ is independent of the parameter r_s . It is also easy to verify that for small values of m , the solution $E_0 = m_Q$ obtained from Eq. (15) is proportional to m , as expected. We can also find out the kinetic mass term with the result:

$$\frac{1}{2M_{kin}} = \left. \frac{dE_{\mathbf{p}}}{d\mathbf{p}^2} \right|_{\mathbf{p}=0} = \frac{\left(1 + \frac{m^2}{4}\right)^2 + m^2 r_s (M_0 + \kappa_t - \kappa_t \cosh E_0)}{(2A \cosh E_0 + B) \sinh E_0} \quad (17)$$

In order to have the usual energy-momentum dispersion relation for the quark, one imposes the condition: $M_{kin} = E_0 \equiv m_Q$ which yields the relationship between χ and κ_t as (restoring the lattice spacing explicitly):

$$\chi^2 = \frac{(A \cosh E_0 + B/2) (\sinh E_0/E_0)}{\left(1 + \frac{m^2}{4}\right)^2 + m^2 r_s (M_0 + \kappa_t - \kappa_t \cosh E_0)}, \quad (18)$$

where the value of $E_0 = m_Q$ is to be obtained from Eq. (15). To summarize, for a given set of parameters χ , M_0 , m and r_s , one has to solve both Eq. (15) and Eq. (18) to obtain the values of κ_t and m_Q .

In Fig. 1, we have shown the pole mass of the quark as a function of the propagator mass parameter: $m_P = m|M_0|$ for a given set of other parameters. Three curves in the plot correspond to $\chi = 1, 3, 5$ respectively. The value of κ_t is obtained from Eq. (18). It is seen that the pole mass of the quark increases with m_P linearly for small values of m_P . For larger values of bare quark mass, some non-linearity sets in.

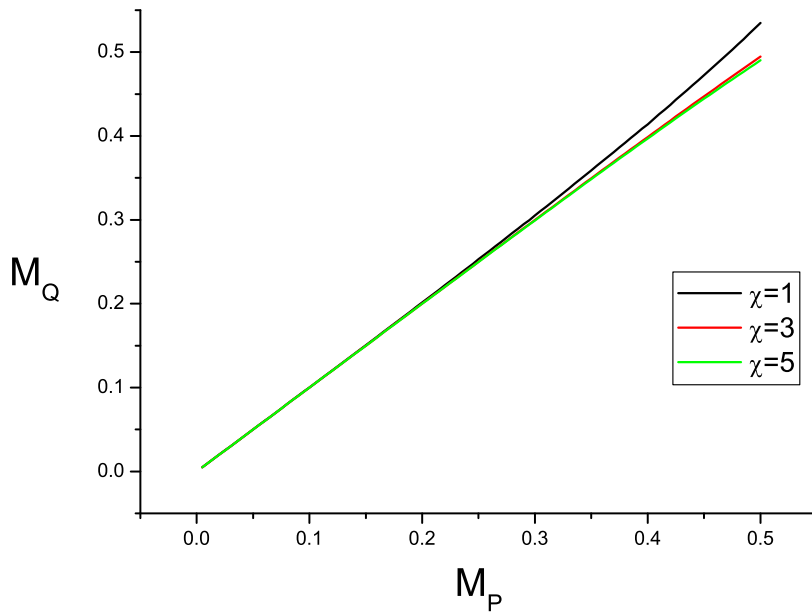


Fig. 1. The pole mass of the free domain wall quark, m_Q , measured in $1/a_s$ unit as a function of the propagator bare mass parameter $m_P = m|M_0|$ for three values of the anisotropy parameter χ . Three curves correspond to $\chi = 1, 3$ and 5 , respectively. We have set $M_0 = -0.5$ and $r_s = 1$ in this plot.

In Fig. 2, for a given value of anisotropy χ , we have plotted the appropriate value of κ_t as a function of the propagator mass parameter m_P . Since m_P is very close to the pole mass m_Q as Fig. 1 indicates, this figure can also be viewed as the dependence of κ_t on m_Q for a given anisotropy χ . It is seen that, in the massless limit, i.e. $m_Q \rightarrow 0$, one recovers the naive relation: $\chi = \kappa_t$. However for massive quarks, this relation is distorted with increasing values of the quark mass. The deviation from its massless limit can be as large as 15% for values of $m_P \simeq 0.5$. In quenched Monte Carlo simulations, the anisotropy χ is fixed by the pure gauge sector. Therefore, this figure can be utilized to tune the hopping parameter κ_t accordingly for a given value of the quark mass and the anisotropy. In a non-perturbative Monte Carlo simulation, this tuning process can be performed by demanding physical particles, e.g. the pions, have the correct dispersion relation for small three-momenta. We would like to emphasize that this tuning process is crucial in the simulation of massive quarks since, without it, the hadrons will not have the correct continuum limit.

In both Fig. 1 and Fig. 2 we have chosen the Wilson parameters r_s to be unity. In principle, other values are also permitted as long as the doublers are well separated from the physical modes. It is seen from Eq. (9b) that the separation between the doublers and the normal physical quark is characterized by the Wilson parameter r_s . Therefore, to decouple the doublers it is better not to

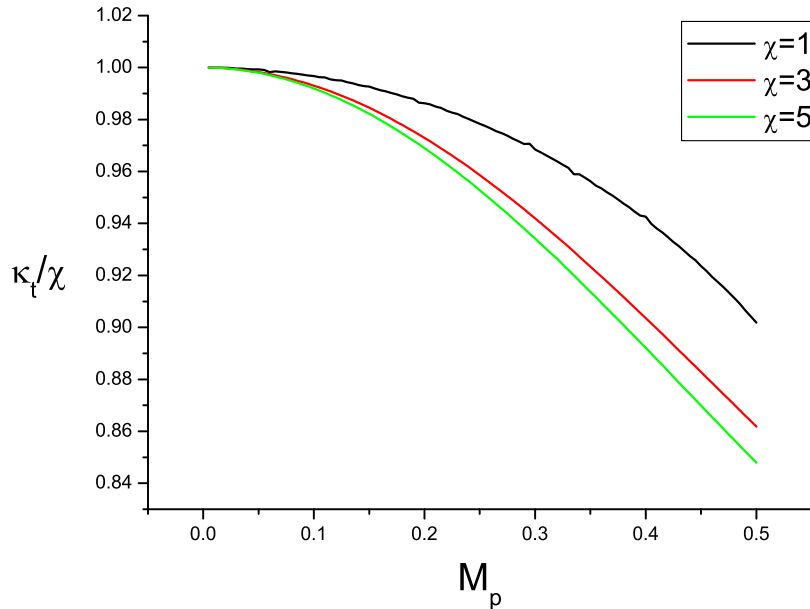


Fig. 2. With the same set of parameters as Fig. 1, the value of κ_t/χ is shown as a function of the propagator mass parameter m_P for $\chi = 1, 3$ and 5 . It is seen that in the massless limit, the expected relation: $\chi = \kappa_t$ is recovered for all χ .

take too small values for r_s . In the remaining part of this paper, we will take the conventional choice: $r_t = r_s = 1$.

4 The wave function and quark mass renormalization to one-loop

In this section, we will compute the quark self-energy to one-loop using bare perturbation theory. Two diagrams contribute at this level: the tadpole diagram and the half-circle diagram. We will first list the necessary Feynman rules and the calculation of these two diagrams will be dealt with afterwards.

4.1 Feynman rules

First of all, one needs the free propagator of the lattice gauge fields [29]. After performing Fourier transformation of the gauge fields, the quadratic part of the gauge action has the standard form in momentum space:

$$S_g^{(0)}[A_\mu] = \frac{1}{2} \sum_{\mu\nu} \int_{-\pi}^{\pi} \frac{d^4 l}{(2\pi)^4} \left(\bar{A}_\mu(l) M_{\mu\nu}(l) \bar{A}_\nu(-l) \right), \quad (19)$$

where

$$M_{00} = \chi \left[\frac{\chi^2 \hat{l}_0^2}{\alpha_g} + \sum_j \hat{l}_j^2 q_{0j} \right] \quad (20)$$

$$M_{jj} = \frac{1}{\chi} \left[\frac{1}{\alpha_g} \hat{l}_j^2 + \chi^2 \hat{l}_0^2 q_{0j} + \sum_{j' \neq j} \hat{l}_{j'}^2 q_{j'j} \right] \quad (21)$$

$$M_{i \neq j} = \frac{1}{\chi} \left[\frac{1}{\alpha_g} \hat{l}_i \hat{l}_j - \hat{l}_i \hat{l}_j q_{ij} \right] \quad (22)$$

$$M_{0j} = M_{j0} = \chi \left[\frac{1}{\alpha_g} \hat{l}_0 \hat{l}_j - \hat{l}_0 \hat{l}_j q_{0j} \right] \quad (23)$$

with lattice momentum defined as: $\hat{l}_\mu \equiv 2 \sin(\frac{l_\mu}{2})$. The quantities $q_{\mu\nu}$ appearing in the above equations are given by:

$$q_{0j} = 1 + \frac{1}{12} \hat{l}_j^2, \quad q_{ij} = 1 + \frac{1}{12} (\hat{l}_i^2 + \hat{l}_j^2) \quad i \neq j. \quad (24)$$

Using these notations, the free gluon propagator is expressed as:

$$D_{\mu\nu}(l) = M_{\mu\nu}^{-1} = \frac{1}{(\hat{l}^2)^2} \left[\alpha_g \hat{l}_\mu \hat{l}_\nu \chi + \frac{f^{\mu\nu}(\hat{l}_\rho, q_{\rho\sigma}, \chi)}{f_D(\hat{l}_\rho, q_{\rho\sigma}, \chi)} \right], \quad (25)$$

The explicit expressions for $f^{\mu\nu}$ and f_D maybe found in the literature [29]. For simplicity, in the following calculation we choose the gauge in which $\alpha_g = 1$.

The vertex functions for the interaction between the quark and the gluon fields can also be obtained with the help of Eq. (7) and Eq. (8). The explicit expressions are given in Eq. (A.1) and Eq. (A.2) in the appendix.

4.2 The half-circle diagram

For the half-circle diagram, the contribution to the quark self-energy can be written as:

$$\begin{aligned} \Sigma^{\text{half-circle}}(p) &= g_0^2 C_F \int \frac{d^4 k}{(2\pi)^4} \sum_\mu \frac{\left(1 - \frac{m}{2}\right)^2}{\{\omega(k) + \omega(p)\}^2} \\ &\quad \times \left\{ \frac{1}{2} \frac{\sigma_\mu^{(1)}(p, k)}{\left(1 + \frac{m^2}{4}\right) \omega(k) + \left(1 - \frac{m^2}{4}\right) b(k)} \right\} D_{\mu\mu}(p - k), \quad (26) \end{aligned}$$

where

$$\begin{aligned}
\sigma_\mu^{(1)}(p, k) &= \left\{ V_{1\mu} \left(\frac{p+k}{2} \right) - \frac{X_0(p)}{\omega(p)} V_{1\mu}^\dagger \left(\frac{p+k}{2} \right) \frac{X_0(k)}{\omega(k)} \right\} \\
&\times \left\{ \left(1 - \frac{m}{2} \right) X_0^\dagger(k) + \left(1 + \frac{m}{2} \right) \omega(k) \right\} \\
&\times \left\{ V_{1\mu} \left(\frac{p+k}{2} \right) - \frac{X_0(k)}{\omega(k)} V_{1\mu}^\dagger \left(\frac{p+k}{2} \right) \frac{X_0(p)}{\omega(p)} \right\}, \tag{27}
\end{aligned}$$

and $D_{\mu\mu}$ is the gluon propagator given in Eq. (25).

We will be interested in the small p behavior of the self-energy. Therefore, one can expand the integrand in Eq. (26) around $p = 0$. Note that $\omega(p)$ is an even function of p . Therefore, when expanded around $p = 0$, one has: $\omega(p) = \omega(0) + O(p^2)$. However, both $D_{\mu\mu}(p-k)$ and $\sigma_\mu^{(1)}(p, k)$ contains terms that are linear in p . When expanding the function $D_{\mu\mu}(p-k)$, the leading term is an even function of k , the term proportional to p is an odd function of k . Therefore, when multiplied with expansion of the function $\sigma_\mu^{(1)}(p, k)$, only the terms that are even functions of k will give non-zero contributions after the integration over k is performed. For example, if we take $D_{\mu\mu}(k)$, then it suffice to keep only even functions of k in the expansion of $\sigma_\mu^{(1)}(p, k)$:

$$\begin{aligned}
\sigma_\mu^{(1)}(0, k) &= \left\{ V_{1\mu} \left(\frac{k}{2} \right) + V_{1\mu}^\dagger \left(\frac{k}{2} \right) \frac{X_0(k)}{\omega(k)} \right\} \\
&\times \left\{ \left(1 - \frac{m}{2} \right) X_0^\dagger(k) + \left(1 + \frac{m}{2} \right) \omega(k) \right\} \\
&\times \left\{ V_{1\mu} \left(\frac{k}{2} \right) + \frac{X_0(k)}{\omega(k)} V_{1\mu}^\dagger \left(\frac{k}{2} \right) \right\}, \\
&\sim \left\{ \left(1 - \frac{m}{2} \right) \omega + \left(1 + \frac{m}{2} \right) b \right\} \\
&\times \left(V_{1\mu}^\dagger V_{1\mu} + V_{1\mu} V_{1\mu}^\dagger + \frac{2}{\omega} V_{1\mu}^\dagger X_0 V_{1\mu}^\dagger \right). \tag{28}
\end{aligned}$$

Here the symbol “ \sim ” means that the odd functions of k are dropped from the expression. Similarly, if the terms linear in p from $D_{\mu\mu}(p-k)$ are taken, which is an odd function of k , then only terms that are odd functions of k in the expansion of $\sigma_\mu^{(1)}(p, k)$ will contribute to the integral.

Then, we calculate the quantity $d\sigma_\nu^{(1)}(p, k)/dp_\mu$. First, we notice that

$$\left. \frac{dV_{1\nu} \left(\frac{p+k}{2} \right)}{dp_\mu} \right|_{p=0} = -\frac{i}{2} \gamma_\mu V_{1\nu} \left(\frac{k}{2} \right) \delta_{\mu\nu}, \quad \left. \frac{dX_0(p)}{dp_\mu} \right|_{p=0} = i\kappa_\mu \gamma_\mu. \tag{29}$$

We define: $d\sigma_\nu^{(1)}(p, k)/dp_\mu \equiv i\kappa_\mu \gamma_\mu \sigma_\mu^{(1)\nu}$ and the explicit calculation shows:

$$\begin{aligned}
\left. \frac{d\sigma_\nu^{(1)}(p, k)}{dp_\mu} \right|_{p=0} &= \left\{ -\frac{i}{2} \gamma_\mu V_{1\mu} \left(\frac{k}{2} \right) \delta_{\mu\nu} + i \gamma_\mu \frac{\kappa_\mu}{M_0} V_{1\nu}^\dagger \left(\frac{k}{2} \right) \frac{X_0(k)}{\omega(k)} \right. \\
&\quad \left. + \frac{i}{2} \gamma_\mu V_{1\mu}^\dagger \left(\frac{k}{2} \right) \frac{X_0(k)}{\omega(k)} \delta_{\mu\nu} \right\} \\
&\times \left\{ \left(1 - \frac{m}{2} \right) X_0^\dagger(k) + \left(1 + \frac{m}{2} \right) \omega(k) \right\} \\
&\times \left\{ V_{1\nu} \left(\frac{k}{2} \right) + \frac{X_0(k)}{\omega(k)} V_{1\nu}^\dagger \left(\frac{k}{2} \right) \right\} \\
&+ \left\{ V_{1\nu} \left(\frac{k}{2} \right) + V_{1\nu}^\dagger \left(\frac{k}{2} \right) \frac{X_0(k)}{\omega(k)} \right\} \\
&\times \left\{ \left(1 - \frac{m}{2} \right) X_0^\dagger(k) + \left(1 + \frac{m}{2} \right) \omega(k) \right\} \\
&\times \left\{ -\frac{i}{2} \gamma_\mu V_{1\mu} \left(\frac{k}{2} \right) \delta_{\mu\nu} + \frac{X_0(k)}{\omega(k)} V_{1\nu}^\dagger \left(\frac{k}{2} \right) i \gamma_\mu \frac{\kappa_\mu}{M_0} \right. \\
&\quad \left. + \frac{X_0(k)}{\omega(k)} V_{1\mu}^\dagger \left(\frac{k}{2} \right) \frac{i}{2} \gamma_\mu \delta_{\mu\nu} \right\}. \tag{30}
\end{aligned}$$

As we clarified before, we only need to keep odd functions of k in this quantity. Thus we get:

$$\begin{aligned}
\left. \frac{d\sigma_\nu^{(1)}(p, k)}{dp_\mu} \right|_{p=0} &\sim \left(1 - \frac{m}{2} \right) \left\{ -\frac{i}{2} \{ \gamma_\mu, V_{1\mu} X_0^\dagger V_{1\mu} \} \delta_{\mu\nu} + \frac{i}{2} \{ \gamma_\mu, V_{1\mu}^\dagger X_0 V_{1\mu}^\dagger \} \delta_{\mu\nu} \right. \\
&\quad \left. + i \gamma_\mu \frac{\kappa_\mu}{M_0} \omega (V_{1\nu}^\dagger V_{1\nu} + V_{1\nu} V_{1\nu}^\dagger) + i \frac{\kappa_\mu}{M_0} \{ \gamma_\mu, V_{1\nu}^\dagger X_0 V_{1\nu}^\dagger \} \right\} \\
&+ \left(1 + \frac{m}{2} \right) \left\{ -i \gamma_\mu \omega (V_{1\mu} V_{1\mu} + V_{1\mu}^\dagger V_{1\mu}^\dagger) \delta_{\mu\nu} \right. \\
&\quad \left. + i \frac{b}{\omega} \{ \gamma_\mu, V_{1\mu}^\dagger X_0 V_{1\mu}^\dagger \} \delta_{\mu\nu} + i \gamma_\mu \frac{\kappa_\mu}{M_0} b (V_{1\nu}^\dagger V_{1\nu} + V_{1\nu} V_{1\nu}^\dagger) \right. \\
&\quad \left. - i \gamma_\mu \frac{\kappa_\mu}{M_0} 2\omega V_{1\nu}^\dagger V_{1\nu} + i \frac{\kappa_\mu}{M_0} \frac{2b}{\omega} \{ \gamma_\mu, V_{1\nu}^\dagger X_0 V_{1\nu}^\dagger \} \right\}. \tag{31}
\end{aligned}$$

Here the symbol “ \sim ” means that the even functions of k are dropped from the expression. Using the expressions for various quantities, we have:

$$\begin{aligned}
V_{1\nu}^\dagger V_{1\nu} &= V_{1\nu} V_{1\nu}^\dagger = \kappa_\nu^2 \\
V_{1\nu} V_{1\nu} &\sim -\kappa_\nu^2 \cos k_\nu \quad V_{1\nu}^\dagger V_{1\nu}^\dagger \sim -\kappa_\nu^2 \cos k_\nu \\
V_{1\nu}^\dagger X_0 V_{1\nu}^\dagger &\sim \kappa_\nu^2 (\kappa_\nu \sin^2 k_\nu - b \cos k_\nu) \\
V_{1\nu} X_0^\dagger V_{1\nu} &\sim \kappa_\nu^2 (\kappa_\nu \sin^2 k_\nu - b \cos k_\nu) \tag{32}
\end{aligned}$$

Finally, we calculate the term $dD_{\nu\nu}(p-k)/dp_\mu|_{p=0}$:

$$\begin{aligned} \left. \frac{dD_{\nu\nu}(p-k)}{dp_\mu} \right|_{p=0} &= \hat{k}_\mu \left\{ \frac{4(\chi^2)^{\delta_{\mu 0}}}{\left(\chi^2 \hat{k}_0^2 + \sum_j \hat{k}_j^2\right)^3} \left[\chi \hat{k}_\nu^2 + \frac{f^{\nu\nu}}{f_D} \right] \right. \\ &\quad \left. + \frac{1}{\left(\chi^2 \hat{k}_0^2 + \sum_j \hat{k}_j^2\right)^2} \left[-2\chi \delta_{\mu\nu} - \frac{f_\mu^\nu}{f_D} + \frac{f_\mu^D f^{\nu\nu}}{f_D^2} \right] \right\} \end{aligned} \quad (33)$$

where we have used the following notations:

$$f_\mu^\nu(k) = - \left. \frac{\partial f^{\nu\nu}(p-k)}{\hat{k}_\mu \partial p_\mu} \right|_{p=0}, \quad f_\mu^D(k) = - \left. \frac{\partial f_D(p-k)}{\hat{k}_\mu \partial p_\mu} \right|_{p=0}. \quad (34)$$

As mentioned above, here the even functions of k in $\sigma_\nu^{(1)}(0, k)$ will vanish and the odd ones will survive. These terms are of the following form:

$$\begin{aligned} \hat{k}_\mu \sigma_\nu^{(1)}(0, k) &\sim i\kappa_\mu \gamma_\mu \hat{k}_\mu \sin k_\mu \left\{ 2 \left(1 + \frac{m}{2} \right) \kappa_\mu \omega \delta_{\mu\nu} \right. \\ &\quad \left. + 2 \left(1 + \frac{m}{2} \right) \left(\kappa_\nu^2 \sin^2 \frac{k_\nu}{2} + \kappa_\nu^2 \cos^2 \frac{k_\nu}{2} (2\delta_{\mu\nu} - 1) \right) \right. \\ &\quad \left. + \frac{2b}{\omega} \left(1 + \frac{m}{2} \right) \left(-b\kappa_\mu \delta_{\mu\nu} + \kappa_\nu^2 - 2\kappa_\mu^2 \cos^2 \frac{k_\mu}{2} \delta_{\mu\nu} \right) \right\} \end{aligned} \quad (35)$$

Collecting all the relevant terms, we may write the contribution from the half-circle diagram as:

$$\Sigma^{\text{half-circle}}(p) = g^2 \left(i \sum_\mu \gamma_\mu \tilde{p}_\mu I_\mu^{(1)} + M^{(1)} \right). \quad (36)$$

Introducing the following notations:

$$\left. \frac{d\sigma_\nu^{(1)}(p, k)}{dp_\mu} \right|_{p=0} = i\kappa_\mu \gamma_\mu \bar{\sigma}_\mu^{(1)\nu}(k) \quad \hat{k}_\mu \sigma_\nu^{(1)}(0, k) = i\kappa_\mu \gamma_\mu \tilde{\sigma}_\mu^{(1)\nu}(k), \quad (37)$$

the quantity $I^{(1)}$ and $M^{(1)}$ are expressed in terms of the following integrals:

$$I_\mu^{(1)} = C_F \int \frac{d^4k}{(2\pi)^4} \sum_\nu \frac{\left(1 - \frac{m}{2}\right)^2}{\{\omega - M_0\}^2} \left\{ \frac{1}{2} \frac{1}{\left(1 + \frac{m^2}{4}\right)\omega + \left(1 - \frac{m^2}{4}\right)b} \right\} \\ \times \left(\bar{\sigma}_\mu^{(1)\nu}(k) S_g^{\nu\nu}(k) + \tilde{\sigma}_\mu^{(1)\nu}(k) \frac{dD_{\nu\nu}(p-k)}{\hat{k}_\mu dp_\mu} \Big|_{p=0} \right), \quad (38)$$

$$M^{(1)} = C_F \int \frac{d^4k}{(2\pi)^4} \sum_\mu \frac{\left(1 - \frac{m}{2}\right)^2}{\{\omega - M_0\}^2} \\ \times \left\{ \frac{1}{2} \frac{\sigma_\mu^{(1)}(0, k)}{\left(1 + \frac{m^2}{4}\right)\omega + \left(1 - \frac{m^2}{4}\right)b} \right\} D_{\mu\mu}(k). \quad (39)$$

where all integrations are taken in the first Brillouin zone.

4.3 The tadpole diagram

Using the Feynman rules given in the previous section, the contribution from the tadpole diagram can be written as:

$$\Sigma^{\text{tadpole}}(p) = \frac{1}{2} g^2 C_F \int_{-\pi}^{\pi} \frac{d^4k}{(2\pi)^4} \sum_\mu \left(1 - \frac{m}{2}\right) \sigma_\mu^{(2)}(p, k) D_{\mu\mu}(k), \quad (40)$$

where the function $\sigma_\mu^{(2)}(p, k)$ reads:

$$\sigma_\mu^{(2)}(p, k) = -\frac{1}{2\omega(p)} \left\{ V_{2\mu}(p) - \frac{X_0(p)}{\omega(p)} V_{2\mu}^\dagger(p) \frac{X_0(p)}{\omega(p)} \right\} + \frac{1}{\omega(p) \{\omega(p) + \omega(p+k)\}^2} \\ \times \left\{ X_0(p) V_{1\mu}^\dagger \left(p + \frac{k}{2}\right) V_{1\mu} \left(p + \frac{k}{2}\right) + V_{1\mu} \left(p + \frac{k}{2}\right) X_0^\dagger(p+k) V_{1\mu} \left(p + \frac{k}{2}\right) \right. \\ \left. + V_{1\mu} \left(p + \frac{k}{2}\right) V_{1\mu}^\dagger \left(p + \frac{k}{2}\right) X_0(p) \right. \\ \left. - \frac{2\omega(p) + \omega(p+k)}{\omega(p)^2 \omega(p+k)} X_0(p) V_{1\mu}^\dagger \left(p + \frac{k}{2}\right) X_0(p+k) V_{1\mu}^\dagger \left(p + \frac{k}{2}\right) X_0(p) \right\}. \quad (41)$$

For small lattice momenta p , the function $\sigma_\mu^{(2)}(p, k)$ is expanded. It contains a term at vanishing momentum:

$$\sigma_\mu^{(2)}(0, k) = -\frac{1}{\{\omega - M_0\}^2} \left(V_{1\mu}^\dagger V_{1\mu} + V_{1\mu} V_{1\mu}^\dagger + \frac{2}{\omega} V_{1\mu}^\dagger X_0 V_{1\mu}^\dagger \right), \quad (42)$$

and a term that is linear in p . To evaluate this term, we need $d\sigma_\nu^{(2)}(p, k)/dp_\mu \equiv i\kappa_\mu\gamma_\mu\sigma_\mu^{(2)\nu}$:

$$\begin{aligned}
\left. \frac{d\sigma_\nu^{(2)}(p, k)}{dp_\mu} \right|_{p=0} &= -\frac{i\kappa_\mu\gamma_\mu}{M_0} \left(\delta_{\mu\nu} + \frac{\kappa_\nu}{M_0} \right) - i\kappa_\mu\gamma_\mu \frac{4\kappa_\mu^2 \cos k_\mu + 4\kappa_\mu b}{\{\omega - M_0\}^2 M_0 \omega^2} \sin^2 k_\mu \\
&\times \left\{ -b\kappa_\mu\delta_{\mu\nu} + \kappa_\nu^2 - 2\kappa_\mu^2 \cos^2 \frac{k_\mu}{2} \delta_{\mu\nu} \right\} \\
&- \frac{1}{M_0\{\omega(k) - M_0\}^2} \left[i\kappa_\mu\gamma_\mu (V_{1\nu}^\dagger V_{1\nu} + V_{1\nu} V_{1\nu}^\dagger) \right. \\
&- i\{\gamma_\mu, V_{1\mu} X_0^\dagger V_{1\mu}\} \delta_{\mu\nu} + V_{1\nu} \left. \frac{dX_0^\dagger(p+k)}{dp_\mu} \right|_{p=0} V_{1\nu} \\
&- i\kappa_\mu\gamma_\mu \frac{2\kappa_\mu^2 \cos k_\mu + 2\kappa_\mu b}{\omega^3} \sin^2 k_\mu \\
&\times M_0 \left\{ -b\kappa_\mu\delta_{\mu\nu} + \kappa_\nu^2 - 2\kappa_\mu^2 \cos^2 \frac{k_\mu}{2} \delta_{\mu\nu} \right\} \\
&- \left(\frac{1}{M_0} - \frac{2}{\omega} \right) \left(i\kappa_\mu\{\gamma_\mu, V_{1\nu}^\dagger X_0 V_{1\nu}^\dagger\} + iM_0\{\gamma_\mu, V_{1\mu}^\dagger X_0 V_{1\mu}^\dagger\} \delta_{\mu\nu} \right. \\
&\left. + M_0 V_{1\nu}^\dagger \frac{dX_0(p+k)}{dp_\mu} \Big|_{p=0} V_{1\nu}^\dagger \right) \left. \right]. \tag{43}
\end{aligned}$$

Note that we have:

$$\begin{aligned}
V_{1\nu} \left. \frac{dX_0^\dagger(p+k)}{dp_\mu} \right|_{p=0} V_{1\nu} &\sim -i\kappa_\mu\gamma_\mu \cos k_\mu \kappa_\nu^2 + i\kappa_\mu^3 \gamma_\mu (1 + \cos k_\mu) \delta_{\mu\nu}, \\
V_{1\nu}^\dagger \left. \frac{dX_0(p+k)}{dp_\mu} \right|_{p=0} V_{1\nu}^\dagger &= -V_{1\nu} \left. \frac{dX_0^\dagger(p+k)}{dp_\mu} \right|_{p=0} V_{1\nu}. \tag{44}
\end{aligned}$$

Therefore, if we introduce the following denotation

$$\left. \frac{d\sigma_\nu^{(2)}(p, k)}{dp_\mu} \right|_{p=0} = i\kappa_\mu\gamma_\mu \bar{\sigma}_\mu^{(2)\nu}(k), \tag{45}$$

we can parameterize the contribution from the tadpole diagram as:

$$\Sigma^{\text{tadpole}}(p) = g^2 \left(i \sum_\mu \gamma_\mu \tilde{P}_\mu I_\mu^{(2)} + M^{(2)} \right), \tag{46}$$

where the quantities $I^{(2)}$ and $M^{(2)}$ are given by:

$$I_\mu^{(2)} = \frac{1}{2} C_F \int_{-\pi}^{\pi} \frac{d^4 k}{(2\pi)^4} \sum_\nu \left(1 - \frac{m}{2}\right) \bar{\sigma}_\mu^{(2)\nu}(k) D_{\nu\nu}(k), \quad (47)$$

$$M^{(2)} = \frac{1}{2} C_F \int_{-\pi}^{\pi} \frac{d^4 k}{(2\pi)^4} \sum_\mu \left(1 - \frac{m}{2}\right) \sigma_\mu^{(2)}(0, k) D_{\mu\mu}(k). \quad (48)$$

Adding the contributions from the half circle and the tadpole diagrams together, one can verify that $M^{(1)} + M^{(2)}$ is proportional to the quark mass:

$$M^{(1)} + M^{(2)} = -C_F \int_{-\pi}^{\pi} \frac{d^4 k}{(2\pi)^4} \sum_\mu \frac{m \left(1 - \frac{m}{2}\right)}{\{\omega - M_0\}^2} \times \left\{ \frac{1}{2} \frac{\omega \left(V_{1\mu}^\dagger V_{1\mu} + V_{1\mu} V_{1\mu}^\dagger + \frac{2}{\omega} V_{1\mu}^\dagger X_0 V_{1\mu} \right)}{\left(1 + \frac{m^2}{4}\right) \omega + \left(1 - \frac{m^2}{4}\right) b} \right\} D_{\mu\mu}(k). \quad (49)$$

This is the expected result since it is known that quark mass is only multiplicative renormalized in QCD due to chiral symmetry. In what follows, we will define:

$$M^{(3)} = \frac{M^{(1)} + M^{(2)}}{m_P}, \quad (50)$$

which is a finite quantity in the chiral limit.

4.4 The massless case

If the quark mass is exactly zero, then the one-loop contribution discussed above contains infra-red divergences. However, the same infra-red divergence also exists in the continuum. Therefore, one can subtract an appropriate infra-red divergent part from the one-loop contribution:

$$I_{\text{finite},\mu}^{(1)} = I_\mu^{(1)}(m=0) - \frac{C_F}{M_0} \int_{-\pi}^{\pi} \frac{d^4 k}{(2\pi)^4} \frac{4\chi(\chi^2)^{\delta_{\mu 0}} k_\mu^2 \theta(\pi^2 - (\chi^2 k_0^2 + \sum_j k_j^2))}{(\chi^2 k_0^2 + \sum_j k_j^2)^3} \quad (51)$$

$$I_{\text{log},\mu}^{(1)} = \frac{C_F}{16\pi^2 M_0} \left(\ln(\pi^2) + 1 - \ln(\tilde{p}^2) \right) \quad (52)$$

$$M_{\text{finite}}^{(3)} = M^{(3)}(m=0) - \frac{C_F}{M_0} \int_{-\pi}^{\pi} \frac{d^4 k}{(2\pi)^4} \frac{4\chi\theta(\pi^2 - (\chi^2 k_0^2 + \sum_j k_j^2))}{(\chi^2 k_0^2 + \sum_j k_j^2)^2} \quad (53)$$

$$M_{\text{log}}^{(3)} = \frac{C_F}{4\pi^2 M_0} \left(\ln(\pi^2) + 1 - \ln(\tilde{p}^2) \right) \quad (54)$$

The subtracted contributions listed above are all infra-red finite. Therefore they can be evaluated numerically once the bare parameters are fixed. The infra-red divergent part can be obtained analytically and depends on the external momentum (or a scale parameter when external momentum is vanishing) as usual.

4.5 Numerical results

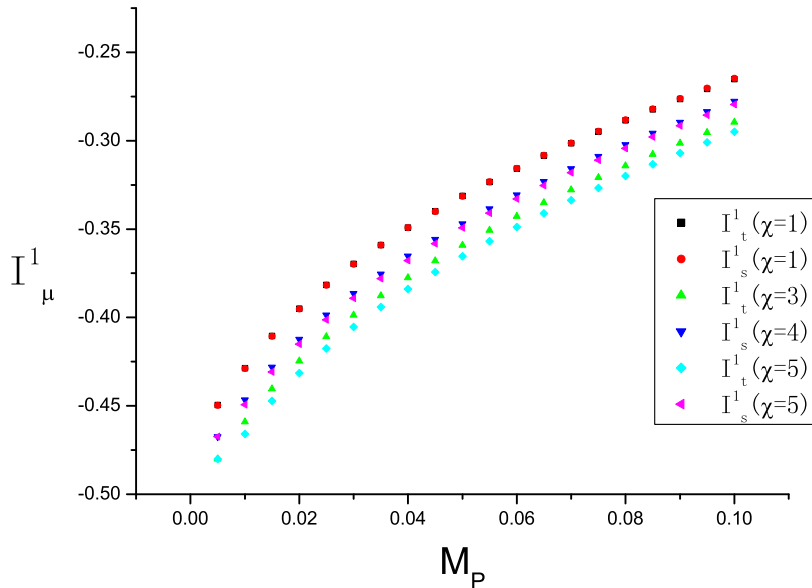


Fig. 3. The values of $I_\mu^{(1)}(m)$ as a function of m_P are shown for $\chi = 1, 3$ and 5 . Here $I_t^{(1)}$ corresponds to $\mu = 0$ and $I_s^{(1)}$ corresponds to $\mu = 1, 2, 3$. Other bare parameters are: $\kappa_s = 1$, $M_0 = -0.5$.

As we pointed out above, if the quark mass is non-zero, quantities $I_\mu^{(1)}(m)$, $I_\mu^{(2)}(m)$ and $M^{(3)}(m)$ can be calculated directly using numerical integration once the bare parameters are given. In Fig. 3 and Fig. 4, we have shown the values of $I_\mu^{(1)}$ and $I_\mu^{(2)}$ as functions of the propagator mass parameter m_P . Here the subscript “t” corresponds to $\mu = 0$ and the subscript “s” corresponds to $\mu = 1, 2, 3$. In Fig. 5, we have shown the values of $M^{(3)}$ as a function of the propagator mass parameter m_P .

In the massless case, the subtracted part of the loop integrals can be computed numerically following Eq. (51) and Eq. (53). Since the main purpose of this paper is to address massive overlap quarks, we will not list the numerical results for the massless case.

Finally, our calculation can be easily translated into its tadpole-improved ver-

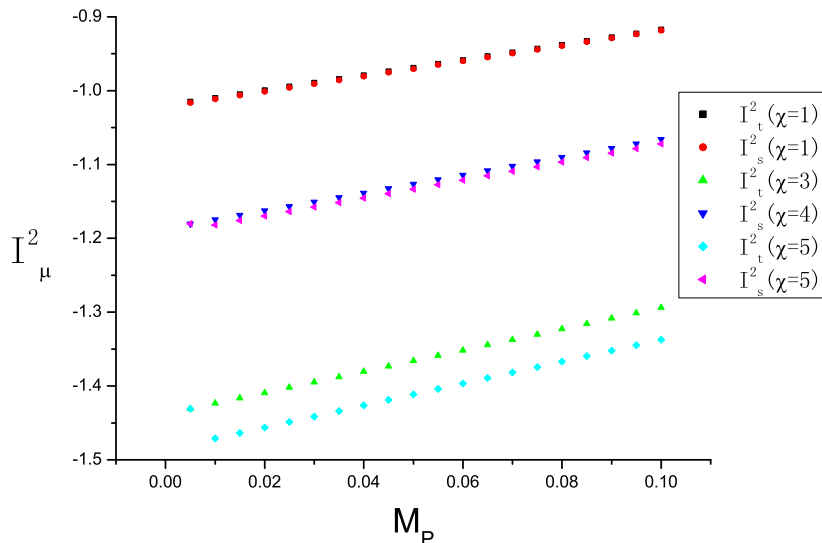


Fig. 4. The values of $I_\mu^{(2)}(m)$ as a function of m_P are shown for $\chi = 1, 3$ and 5 . Here $I_t^{(1)}$ corresponds to $\mu = 0$ and $I_s^{(1)}$ corresponds to $\mu = 1, 2, 3$. Other bare parameters are: $\kappa_s = 1$, $M_0 = -0.5$.

sion following standard steps. For example, if we use the mean-field estimate (tree-level tadpole improved theory), Eq. (9b) is modified to:

$$\tilde{b}(p) = \sum_{\mu} \kappa_{\mu} (1 - u_{\mu} \cos p_{\mu}) + M_0, \quad (55)$$

where u_{μ} represents the mean-field value for the gauge field U_{μ} . Note that for small lattice momenta, this amounts to a shift in parameter M_0 :

$$\tilde{M}_0 = M_0 + \sum_{\mu} \kappa_{\mu} (1 - u_{\mu}). \quad (56)$$

Similarly, the tuning of the hopping parameter κ_t can also be discussed within the mean-field approximation. Note that these might be a rather good estimate for the correct value for the parameters in future Monte Carlo simulations.

5 Discussions and conclusions

In this paper, we have studied massive overlap fermions on anisotropic lattices. We argue that this setup can be useful in many lattice QCD studies. It is shown that, in order to restore the usual dispersion relation for the quark at small three-momenta, hopping parameter κ_t has to be tuned according to the quark mass values. Quark propagator is calculated using bare perturbation theory to one-loop order. We find the wave-function and mass renormalization constants

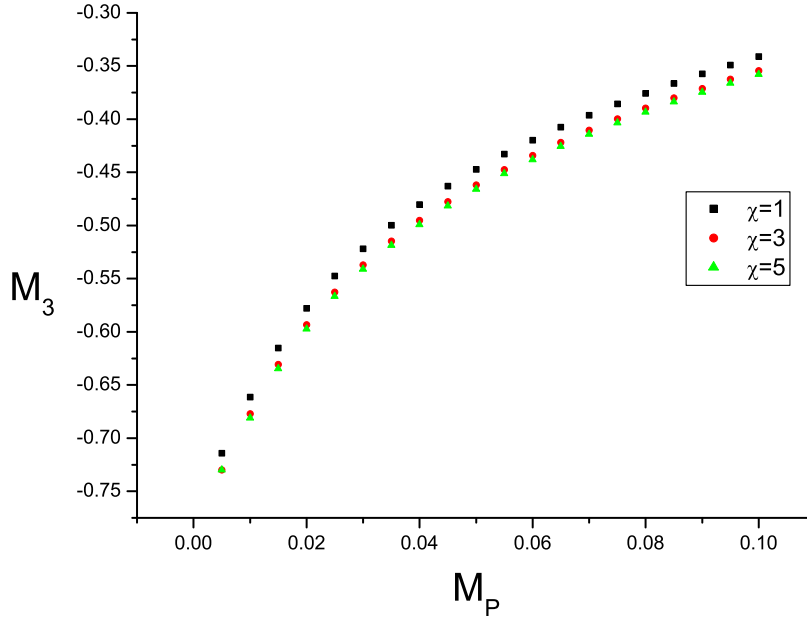


Fig. 5. The values of $M^{(3)}(m)$ as a function of m_P are shown for $\chi = 1, 3$ and 5 . Other bare parameters are: $\kappa_s = 1$, $M_0 = -0.5$.

at various values of the bare parameters. These results serve as a guidance for the tuning of the parameters in real Monte Carlo simulations.

A Vertex functions

Here we list the vertex functions used in the main text. The isotropic lattice counterparts for the vertex functions can be found in the literature [21,22,23,24] and the version for anisotropic lattice can be obtained accordingly after obvious modifications. The interaction vertex for the quark field, anti-quark field and one gluon field reads:

$$-g_0 \frac{1 - \frac{m}{2}}{\omega(q) + \omega(p)} T_{ab}^A \left\{ V_{1\mu} \left(p + \frac{k}{2} \right) - \frac{X_0(q)}{\omega(q)} V_{1\mu}^\dagger \left(p + \frac{k}{2} \right) \frac{X_0(p)}{\omega(p)} \right\}. \quad (\text{A.1})$$

The two-gluon interaction vertex is much more complicated. It is found to be:

$$\begin{aligned}
& -g_0^2 \left(1 - \frac{m}{2}\right) \frac{1}{2} \{T^A, T^B\}_{ab} \times \\
& \left[\frac{1}{\omega(q) + \omega(p)} \left\{ V_{2\mu} \left(p + \frac{k}{2}\right) \delta_{\mu\nu} - \frac{X_0(q)}{\omega(q)} V_{2\mu}^\dagger \left(p + \frac{k}{2}\right) \frac{X_0(p)}{\omega(p)} \delta_{\mu\nu} \right\} \right. \\
& \quad \frac{1}{\{\omega(q) + \omega(p)\} \{\omega(p) + \omega(p + k_1)\} \{\omega(p + k_1) + \omega(q)\}} \\
& \quad \times \left\{ X_0(q) V_{1\mu}^\dagger \left(p + k_2 + \frac{k_1}{2}\right) V_{1\nu} \left(p + \frac{k_2}{2}\right) \right. \\
& \quad + V_{1\mu} \left(p + k_2 + \frac{k_1}{2}\right) X_0^\dagger(p + k_2) V_{1\nu} \left(p + \frac{k_2}{2}\right) \\
& \quad + V_{1\mu} \left(p + k_2 + \frac{k_1}{2}\right) V_{1\nu}^\dagger \left(p + \frac{k_2}{2}\right) X_0(p) \\
& \quad \left. - \frac{\omega(q) + \omega(p) + \omega(p + k_2)}{\omega(q)\omega(p)\omega(p + k_2)} \times \right. \\
& \quad \left. X_0(q) V_{1\mu}^\dagger \left(p + k_2 + \frac{k_1}{2}\right) X_0(p + k_2) V_{1\nu}^\dagger \left(p + \frac{k_2}{2}\right) X_0(p) \right\} \\
& \quad \frac{1}{\{\omega(q) + \omega(p)\} \{\omega(p) + \omega(p + k_1)\} \{\omega(p + k_1) + \omega(q)\}} \\
& \quad \times \left\{ X_0(q) V_{1\nu}^\dagger \left(p + k_1 + \frac{k_2}{2}\right) V_{1\mu} \left(p + \frac{k_1}{2}\right) \right. \\
& \quad + V_{1\nu} \left(p + k_1 + \frac{k_2}{2}\right) X_0^\dagger(p + k_1) V_{1\mu} \left(p + \frac{k_1}{2}\right) \\
& \quad + V_{1\nu} \left(p + k_1 + \frac{k_2}{2}\right) V_{1\mu}^\dagger \left(p + \frac{k_1}{2}\right) X_0(p) \\
& \quad \left. - \frac{\omega(q) + \omega(p) + \omega(p + k_1)}{\omega(q)\omega(p)\omega(p + k_1)} \times \right. \\
& \quad \left. X_0(q) V_{1\nu}^\dagger \left(p + k_1 + \frac{k_2}{2}\right) X_0(p + k_1) V_{1\mu}^\dagger \left(p + \frac{k_1}{2}\right) X_0(p) \right\} \Big]. \quad (A.2)
\end{aligned}$$

References

- [1] D. Kaplan. A method for simulating chiral fermions on the lattice. *Phys. Lett. B*, 288:342, 1992.
- [2] Y. Shamir. Chiral fermions from lattice boundaries. *Nucl. Phys. B*, 406:90, 1993.
- [3] R. Narayanan and H. Neuberger. Chiral fermions on the lattice. *Phys. Rev. Lett.*, 71:3251, 1993.

- [4] R. Narayanan and H. Neuberger. Chiral determinant as an overlap of two vacua. *Nucl. Phys. B*, 412:574, 1994.
- [5] Herbert Neuberger. Vectorlike gauge theories with almost massless fermions on the lattice. *Phys. Rev. D*, 57(9):5417–5433, May 1998.
- [6] H. Neuberger. Exactly massless quarks on the lattice. *Phys. Lett. B*, 417:141, 1998.
- [7] H. Neuberger. More about exactly massless quarks on the lattice. *Phys. Lett. B*, 427:353, 1998.
- [8] C. Morningstar and M. Peardon. The glueball spectrum from an anisotropic lattice study. *Phys. Rev. D*, 60:034509, 1999.
- [9] C. Liu. A lattice study of the glueball spectrum. *Chinese Physics Letter*, 18:187, 2001.
- [10] Y. Chen, A. Alexandru, S.J. Dong, T. Draper, I. Horvath, F.X. Lee, K.F. Liu, N. Mathur, C. Morningstar, M. Peardon, S. Tamhankar, B.L. Young, and J.B. Zhang. Glueball spectrum and matrix elements on anisotropic lattices. *Phys. Rev. D*, 73:014516, 2006.
- [11] P. Chen. Heavy quarks on anisotropic lattices: The charmonium spectrum. *Phys. Rev. D*, 64:034509, 2001.
- [12] M. Okamoto et al. Charmonium spectrum from quenched anisotropic lattice qcd. *Phys. Rev. D*, 65:094508, 2002.
- [13] A. Juettner and J. Rolf. A precise determination of the decay constant of the ds-meson in quenched qcd. *Phys. Lett. B*, 560:59, 2003.
- [14] R. Lewis, N. Mathur, and R.M. Woloshyn. Charmed baryons in lattice qcd. *Phys. Rev. D*, 64:094509, 2001.
- [15] C. Liu, J. Zhang, Y. Chen, and J.P. Ma. Calculating the $i=2$ pion scattering length using tadpole improved clover wilson action on coarse anisotropic lattices. *Nucl. Phys. B*, 624:360, 2002.
- [16] G. Meng, C. Miao, X. Du, and C. Liu. Lattice study on kaon nucleon scattering length in the $i=1$ channel. *hep-lat/0309048*, 2003.
- [17] C. Miao, X. Du, G. Meng, and C. Liu. Lattice study on kaon pion scattering length in the $i = 3/2$ channel. *hep-lat/0403028*, 2004.
- [18] X. Du, C. Miao, G. Meng, and C. Liu. $i = 2$ pion scattering length with improved actions on anisotropic lattices. *hep-lat/0404017*, 2004.
- [19] Xu Feng, Xin Li, Wei Liu, and Chuan Liu. Massive domain wall fermions on four-dimensional anisotropic lattices. *JHEP*, 08:060, 2006.
- [20] C. Morningstar and M. Peardon. Efficient glueball simulations on anisotropic lattices. *Phys. Rev. D*, 56:4043, 1997.

- [21] Atsushi Yamada. Weak coupling expansion of a chiral gauge theory on a lattice in the overlap formulation. *Nucl. Phys. B*, 514:399, 1998.
- [22] Y. Kikukawa and A. Yamada. Weak coupling expansion of massless qcd with a ginsparg-wilson fermion and axial u(1) anomaly. *Phys. Lett. B*, 448:265, 1999.
- [23] M. Ishibashi, Y. Kikukawa, T. Noguchi, and A. Yamada. One-loop analyses of lattice qcd with the overlap dirac operator. *Nucl. Phys. B*, 576:501, 2000.
- [24] Kazuo Fujikawa and Masato Ishibashi. A perturbative study of a general class of lattice dirac operators. *Phys. Rev. D*, 65:114504, 2002.
- [25] K.F. Liu and S.J. Dong. Heavy and light quarks with lattice chiral fermions. *Int.J.Mod.Phys. A*, 20:7241, 2002.
- [26] P.H. Ginsparg and K.G. Wilson. A remnant of chiral symmetry on the lattice. *Phys. Rev.*, D25:2649, 1982.
- [27] M. Lüscher. Exact chiral symmetry on the lattice and the ginsparg-wilson relation. *Phys. Lett. B*, 428:342, 1998.
- [28] P. Hasenfratz. Lattice qcd without tuning, mixing and current renormalization. *Nucl. Phys. B*, 525:401, 1998.
- [29] Stefan Groote and Junko Shigemitsu. One-loop self energy and renormalization of the speed of light for some anisotropic improved quark actions. *Phys. Rev. D*, 62:014508, 2000.